An ultra-wide band low-SAR flexible metasurface-enabled antenna for WBAN applications

Husnu Yalduz[1,2,3] · Burak Koç[1,4] · Lokman Kuzu[5] · Mustafa Turkmen[1,2,6]

Abstract

In this study, an ultra-wideband low-specific absorption rate (SAR) flexible metasurface-enabled wearable antenna is proposed for wireless body area network applications. The antenna and metamaterial (MM) structure were designed and analyzed using a commercial electromagnetic simulation software program which uses a finite integration technique solver. The antenna is designed and fabricated on a jeans textile substrate in the size of $58 \times 80 \times 1 \ mm^3$. Moreover, MM reflector was designed on a felt textile substrate to reduce the SAR effect of the antenna and to increase the antenna performance (such as impedance matching, radiation pattern, and realized gain) parameters. Designed and fabricated antenna parameters and the SAR value results with and without MM are investigated. The simulated peak SAR values when the antenna with MM is placed on the body model are 0.86, 0.198, and 0.103 W/kg at frequencies of 4 GHz, 7 GHz, and 10 GHz, respectively, for 10 g of tissue. The simulated peak SAR value of the antenna with MM is also reduced by a percentage of 97, compared to the simulated peak SAR value of the antenna without MM. The peak SAR values of the antenna were less than the European safety limit of 2 W/kg for 10 g of tissue when the MM was used as an isolator. Furthermore, the simulated peak realized gain value of the antenna with the MM was increased by 98% (from 4.6 to 9.1 dB) compared to the simulated peak realized gain value of the antenna without MM. Simulation and measurement results showed that performance characteristics and peak SAR values of the proposed antenna were suitable and safe for wearable technologies.

1 Introduction

In recent years, with the rapid development of wireless communication systems, the area of wireless body area networks (WBANs) has become an influential part of research due to its applications in a wide variety of areas such as health monitoring, patient tracking, rescue systems, battlefield survival, sport, navigation, wearable computing, and so on [1–5]. The wearable antenna is the most important part in WBAN systems, establishing a suitable link between in-body, on-body and off-body devices [6]. Various frequency bands, including ultra-wideband (UWB) and narrowband, have been identified to provide this connection [7]. However, the UWB technology is a more popular solution for the WBAN applications compared to other conventional narrowband wireless communication systems due to some obvious advantages [8]. These advantages can be listed as high data transmission rate, low-power spectral density (− 41.3 dBm/MHz) and low interference [9]. The low-power spectral density is a very attractive feature for wearable battery-operated devices [10]. Another important advantage is using the wide band frequency spectrum of 7.5 GHz from 3.1 to 10.6 GHz which is assigned by Federal Communications Commission (FCC) in 2002 [11]. Therefore the UWB is a new standard for high-speed short-distance wireless communication technologies.

Flexible, textile patch antennas are attractive choices for wearable systems due to their characteristics such as low

✉ Mustafa Turkmen
  turkmen@erciyes.edu.tr

1. Department of Electrical and Electronics Engineering, Erciyes University, 38039 Kayseri, Turkey

2. Fotonik Technology and Engineering, Erciyes Technopark A.S., Yildirim Beyazit Mah. Asik Veysel Bulv. No: 67-3/41, 38039 Kayseri, Turkey

3. Electronics and Automation, Hitit University, Voc. High School, 19169 Corum, Turkey

4. Institute of Accelerator Technologies, Ankara University, 06830 Golbasi, Ankara, Turkey

5. TUBİTAK Space Technologies Research Institute, METU Campus, 06800 Çankaya, Ankara, Turkey

6. Nokta Detection Technologies R&D Center, Sancaktepe, Istanbul, Turkey

profile, lightweight, highly flexible, easy to manufacture and easy to integrate into the garment. These features provide the basic requirements for wearable systems such as flexibility and compactness for user's convenience [12, 13]. Moreover, the textile materials used for the antenna substrate help to reduce surface wave losses and increase the antenna bandwidth with the very low dielectric constant [14]. Recently, several designs of flexible, textile wearable antennas have been presented for WBAN applications such as the monopole [1, 10], inverted-F [5], substrate-integrated waveguide [3, 13], and reconfigurable antennas [2, 15].

Beside the advantages of the above-mentioned wearable antennas, there are some design challenges. In the wearable antenna design, the mutual coupling between the high permittivity human body and antenna should be considered because the antenna is very close to human body [4, 7]. When the antenna operates in close proximity to human body, the performance parameters of the antenna are affected; such as the input impedance bandwidth, radiation pattern, and efficiency [3, 16, 17]. Furthermore, electromagnetic waves have harmful effects on the users' health; this electromagnetic radiation from the antenna penetrates the tissues of the human body [3, 18–21]. The electromagnetic absorption level in body tissue is defined as the SAR value which is evaluated as the absorption of power per unit mass of body tissue. It could be denoted in term of a watt per kilogram (W/kg) [18, 22]. The SAR value should be limited to the standard value defined by the United States (US) or Europe [5]. One of the effective methods to overcome the mutual coupling between the antenna and the human body is using metamaterials (MMs) as an isolator or reflector in wearable applications due to its compatibility with the low-profile antenna design thus resulting in the lower SAR values [23, 24].

MMs are artificial engineering structures with two unique beneficial properties that are not naturally found [21, 25–27]. The first of MM's unique features is the ability to control the propagation of electromagnetic waves, such as artificial magnetic conductor (AMC), with a zero-phase shift. The second is that it has the feature of electromagnetic band gap (EBG) that can suppress surface waves in all directions [28–30]. In the literature, it has been reported that single narrow band [7, 18, 19], dual band [2, 5, 21, 24, 31], and wideband [32–34] are used to improve antenna performance by decreasing the back radiation and SAR value in wearable applications based on MM.

In this study, design and experimental verification of a flexible wearable textile UWB antenna with MM is proposed for WBAN applications. The proposed antenna is a microstrip line feeding antenna consisting of a combination of square and circular patch in sizes of $58 \times 80 \times 1$ mm^3 jeans substrate. A similar geometric structure was previously investigated in [35] for a 2.4 GHz industrial, scientific and medical (ISM) band. Besides, the MM was designed on a felt textile substrate to reduce the SAR value of the design antenna and to increase the antenna performance parameters. This material improves the gain and the directionality of the antenna. Designed and fabricated antenna performance parameters such as impedance matching, radiation pattern, realized gain and the SAR value are simulated and measured and the results with and without MM structure are investigated. The simulated peak SAR values when the antenna with MM was placed on the body model are 0.86, 0.198, and 0.103 W/kg at frequencies of 4 GHz, 7 GHz, and 10 GHz, respectively, for 10 g of tissue. The simulated peak SAR value of the antenna with metamaterial is also reduced by 97%, compared to the simulated peak SAR value of the antenna without MM. The peak SAR values of the antenna were less than the European safety threshold of 2 W/kg when the MM was used as an isolator. Simulated peak realized gain value of the antenna with MM was increased by 98% (from 4.6 to 9.1 dB) compared to the simulated peak realized gain value of the antenna without the MM. Consequently, obtained results showed that the performance characteristics and the peak SAR values of the proposed antenna were suitable and safe for wearable applications.

2 Design and configuration

The antenna and metamaterial structure were designed and analyzed using a commercial electromagnetic simulation software CST Microwave Studio, which is based on the finite integration technique (FIT) solver [36].

2.1 Antenna design

The antenna is fabricated on jeans substrate in size of 58×80 mm^2 with the thickness of 1 mm, relative permittivity of 1.7 and the loss tangent of 0.026. The properties of the dielectric material affect the antenna performance as it plays an important role in the propagation of electromagnetic waves in the dielectric medium. The loss tangent is indicated as a measure of energy losses in dielectrics and the rate of the imaginary part to real part of permittivity ($\tan\delta = \varepsilon''r/\varepsilon'r$). The patch and the ground plane of the antenna are made up using copper tape with a conductivity of 5.88×107 S/m and a thickness of 0.035 mm. The dielectric permittivity of the copper tape adhesive surface was not taken into account. Antenna patch geometry is a combination of circular and square shapes. The antenna is fed using a 3.5-mm wide microstrip line for the 50 O SMA connector. Figure 1 shows the geometry of the proposed antenna configuration design in CST. Figure 2 shows fabricated microstrip line-fed antenna for WBAN applications.
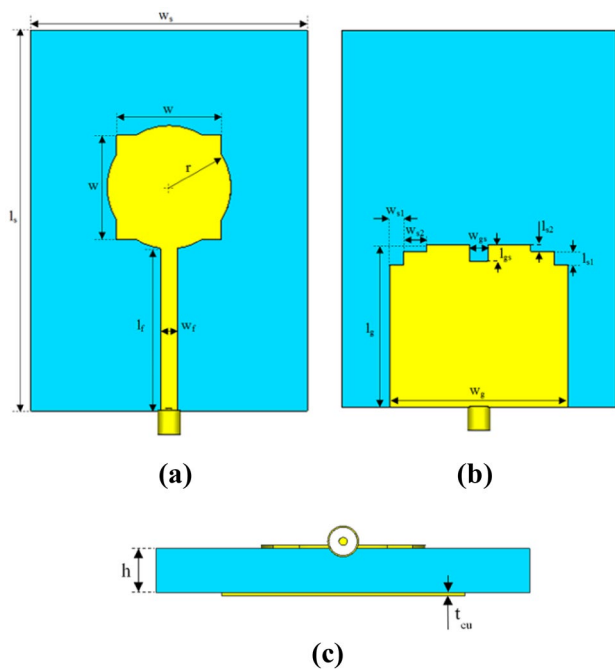
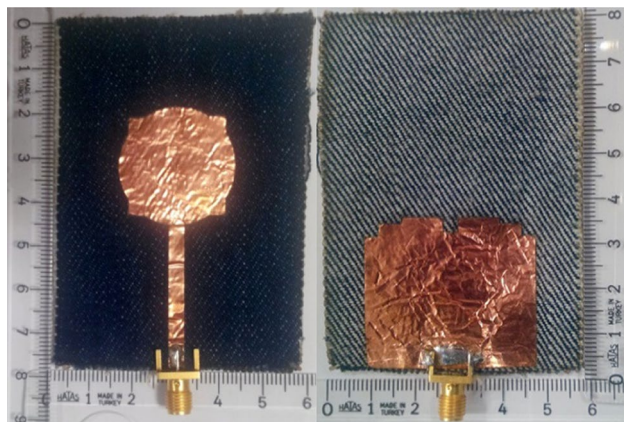**Fig. 1** Configuration of the proposed antenna with; **a** front; **b** back; and **c** bottom view

Fig. 2 Fabricated antenna front and back views

The geometric dimensions of the proposed antenna are given in Table 1.

2.2 Metamaterial design

This sub-section is the design of the MM as the UWB bandwidth reflector to reduce back radiation and to increase antenna gain and directivity. In particular, electromagnetic waves emitted from the antenna can be harmful to body tissues. The MM structure is designed to reduce this SAR effect under the limits of human health. The MM structure is designed by considering the reflection coefficient (S_{11}) parameter of the antenna with MM. The reflection coefficient is a parameter that indicates how much of the power at the antenna input is reflected due to the antenna impedance mismatch and it is used in the antenna design to evaluate the antenna impedance matching and operating frequency band. The ethylene–vinyl acetate (EVA) foam dielectric ($\varepsilon_r = 1.2$, $\tan\delta = 0.005$) material of 3.2 mm thickness was placed as a spacer to maintain the distance and to prevent any electrical contact between the antenna and MM. Figure 3a shows the cross-sectional view of the antenna placed on the MM which consists of three layers: the two metallic (metasurface and ground plane) layers and the dielectric substrate between them. Copper tape with thickness of 0.035 mm was used for metallic layers. The MM structure was designed on felt substrate material with thickness of 3.6 mm, dielectric constant of 1.43 and the tangent loss of 0.044. The geometry of the proposed metasurface structure is shown in Fig. 3b. Due to the ease of fabrication, metasurface unit cell has been chosen in the form of square and consists of 7×7 metasurface array cells. The fabricated prototype of metamaterial is shown in Fig. 3c. The simulated reflection phase graph for optimum MM is given in Fig. 3d. The MM unit cell simulation model in CST is set as the unit cell periodic boundary conditions and the normally incident electromagnetic wave angle with floquet port.

2.3 Body model design

Since wearable antennas work close to the human body, the interaction between the antenna and body tissues is an important issue to be considered. This interaction affected the antenna performance parameters such as impedance matching, radiation pattern, realized gain and directionality. To evaluate the reflection coefficient performance parameter and SAR effect of the antenna on the body, a cubic body model was created in the CST simulation program. As shown in Fig. 4, the body model consists of four layers which are skin-fat-muscle-bone with 2–5 to 20 and 13 mm thickness, respectively [19]. The dielectric properties of the human body tissues are used from the material library in the CST. The total size of the body

	w_f	l_f	w	r	w_g	l_g	w_{gs}	l_{gs}	w_{s1}	l_{s1}	w_{s2}	l_{s2}
Table 1 The geometric dimensions of the proposed antenna (mm)	3.5	34	22	13	37.8	34.4	3.8	3.4	3	3	5	1.4

(a)

(b)

(c)

(d)
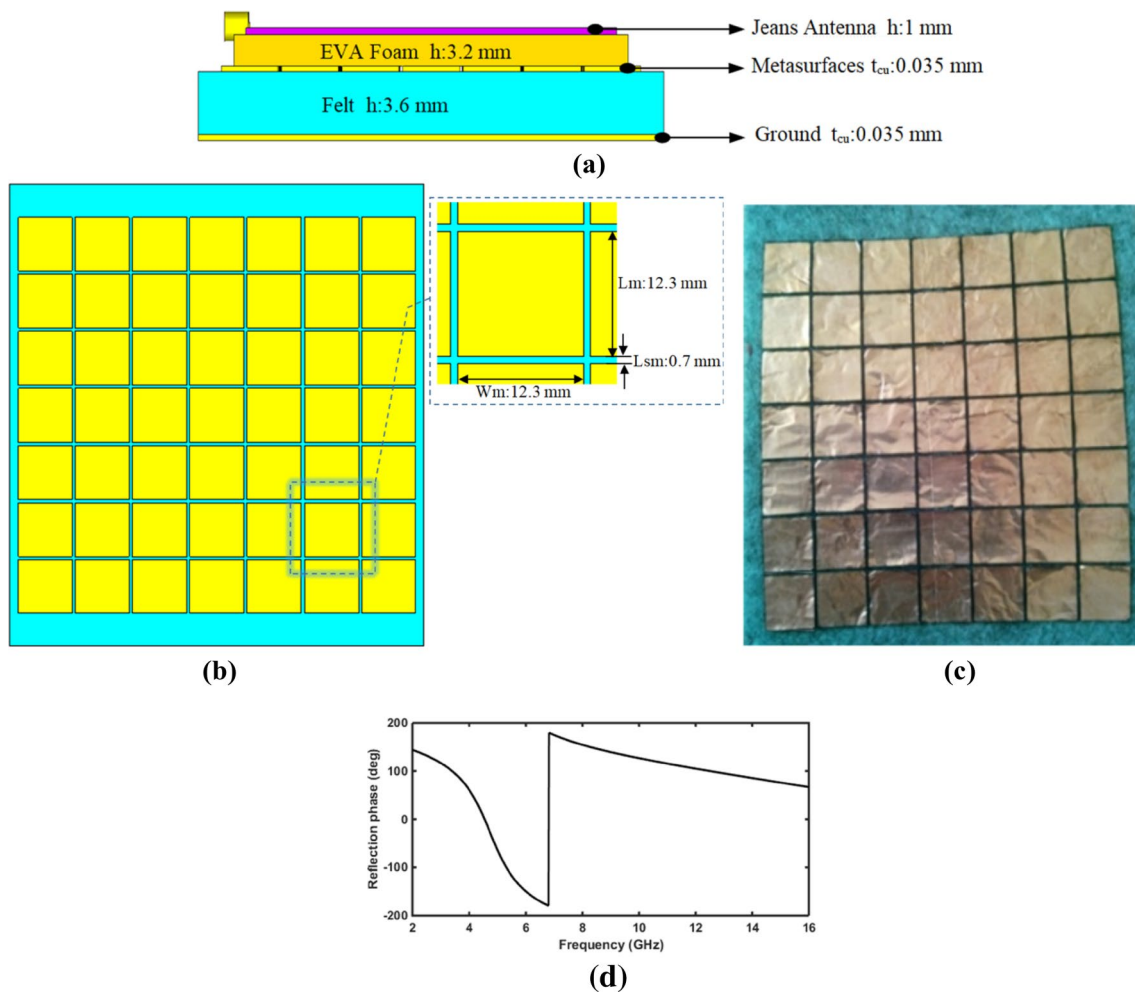
Fig. 3 Configuration of the proposed MM; **a** cross-sectional view of the antenna placed on the MM; **b** geometry of the metasurface structures; **c** fabricated prototype; **d** Reflection phase of MM
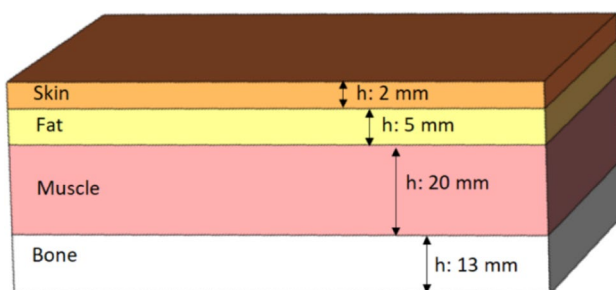

**Fig. 4** Cross-sectional view of the layered cubic human body tissue model

model is $100 \times 110 \times 40$ mm^3. In this study, the reflection coefficient parameter performance and SAR effect of the antenna with and without the MM on the cubic body model are analyzed comparatively by CST. For an objective comparison, the distance between the antenna and the body model was kept constant at 6.9 mm.

3 Experimental results and discussion

The reflection coefficient of the antenna performance parameters is considered as the priority parameter in the design for planar conditions. After this parameter was successfully obtained, the performance of the other parameters was evaluated. The MM structure was designed on the back of the optimum design antenna and the impedance matching of antenna with MM in the design was considered. After the optimum design of MM for the UWB frequency band was obtained in the simulation program, the prototype of the MM was fabricated. Designed and fabricated antenna performance (impedance matching, radiation pattern, and realized gain) parameters and the SAR value simulation and measurement results with and without MM structure are investigated and compared in this section. The reflection coefficient of the antenna prototype was measured by Anritsu MS4644B model Vector Network Analyzer.
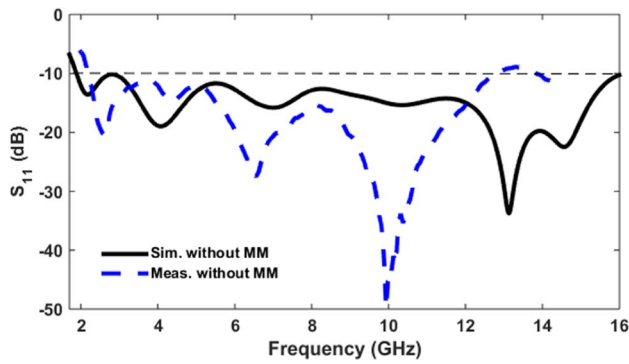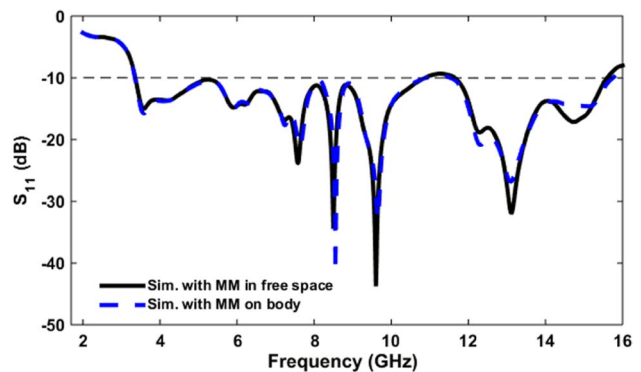
Fig. 5 The simulated and measured S_{11}—parameter graph of the antenna without MM in free space
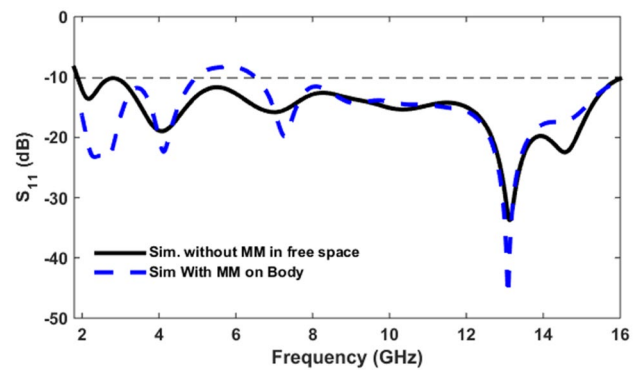
Fig. 7 Simulated S_{11}—parameter graph of the antenna without MM is in the free space and on the body
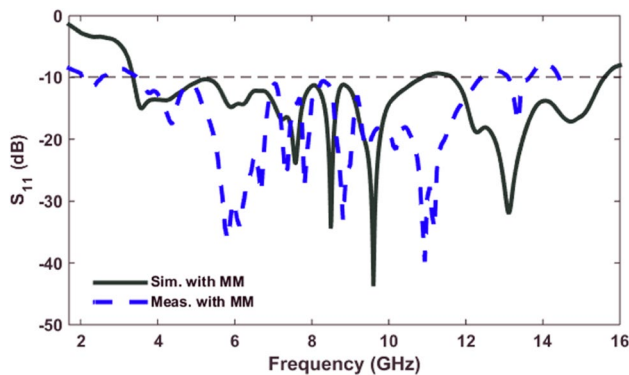
Fig. 6 The simulated and measured S_{11}—parameter graph of the antenna with MM in free space

Fig. 8 Simulated S_{11}—parameter graph of the antenna with MM is in the free space and on the body

3.1 Reflection coefficient of antenna with and without metamaterial structure

The simulation and measurement values of the reflection coefficient parameter of the planar antenna without MM in free space are shown in Fig. 5. The simulated bandwidth was carried out between 1.9 and 16 GHz while the measured bandwidth was carried out between 2.2 and 12.7 GHz. From the simulation and measurement results, it is determined that the proposed antenna has a wide frequency bandwidth, which covers the whole UWB frequency region in free space.

The graph of the simulated and measured reflection coefficient of the MM-integrated antenna in free space is shown in Fig. 6. From the graph, the bandwidth of the simulated result is between 3.4 and 15.8 GHz and the measured result bandwidth of fabricated antenna is between 3.5 and 12.4 GHz. According to the results, the antenna with MM has a good impedance matching (less than − 10 dB) and a wide frequency bandwidth, which is covering the UWB frequency region in the free space.

The differences between the simulation and measurement results in Figs. 5 and 6 can be attributed to manufacturing tolerances, numerical errors, measurement environment, adhesive surface of copper tape and SMA connector soldering effects.

The wearable antenna operates in close proximity to human body, so the reflection coefficient parameter performance of the antenna with and without the MM on the body model is analyzed comparatively by CST. For an objective comparison, the distance between the antenna and the body model was kept constant at 6.9 mm. The simulated reflection coefficient performance results of the antenna with and without MM in the free space and on a cubic body model are given comparatively in Figs. 7 and 8. As a result of the simulation, the reflection coefficient of the antenna without the MM is very different in the free space and on the body. This is because the antenna is affected by the body. Reflection coefficient is higher than − 10 dB from 5 to 6.5 GHz. In addition, the reflection coefficient of the antenna with MM is stable in free space and on-body model. This is because the antenna is isolated from the body by the MM.

Fig. 9 The simulated radiation patterns for the antenna with and without MM (Phi:0 and Phi:90); **a** 4 GHz; **b** 7 GHz; **c** 10 GHz
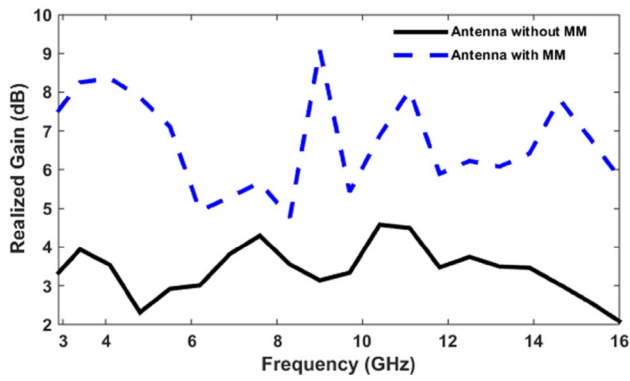

(a)

(b)

(c)
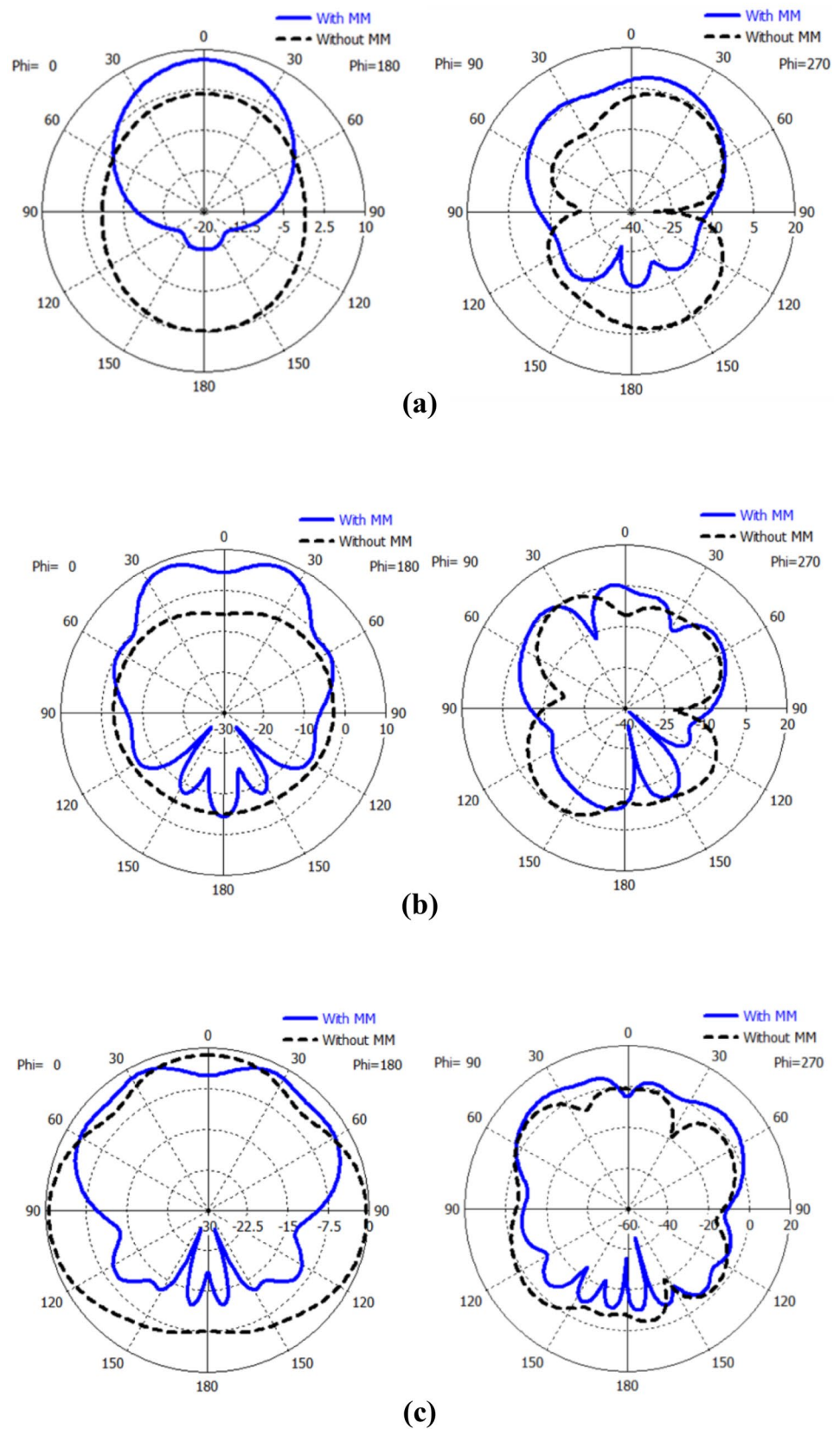
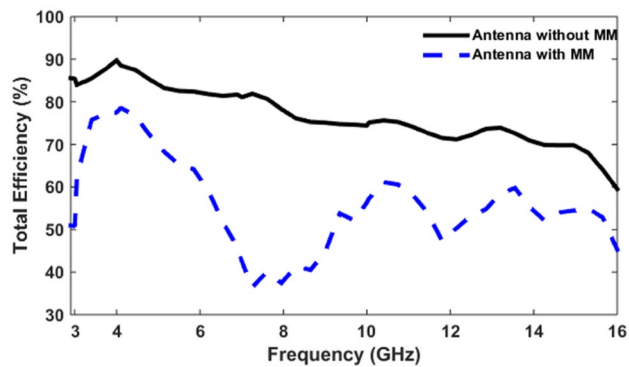**Fig. 10** The simulated realized gain of antenna with and without MM

Fig. 11 The simulated total efficiency of antenna with and without MM
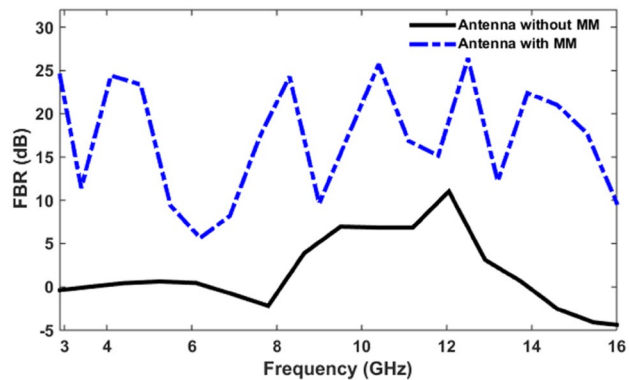

Fig. 12 The simulated front to back ratio (FBR) of antenna with and without MM

## 3.2 Radiation pattern of antenna with and without metamaterial structure

The simulated radiation patterns for the antenna with and without MM are shown comparatively in Fig. 9. These results showed that the back radiation of the MM integrated antenna decreased and thus, the directivity of the antenna is increased.

## 3.3 Realized gain, total efficiency and FBR of antenna with and without metamaterial

In Fig. 10, the simulated realized gain versus frequency graph of the antenna is given comparing antenna with and without MM. It is obvious that the antenna with MM has a higher gain than the antenna without MM over the entire operating frequency band. The realized gain of the antenna without MM varies between 2.1 and 4.6 dB. When the MM is integrated below the antenna, the gain of antenna is above 4.7 dB over the entire operating frequency band. The realized peak gain of the antenna is significantly increased from 4.6 to 9.1 dB. Hence, the peak realized gain value of the antenna with the MM was significantly increased by 98% compared to the peak realized gain value of the antenna without the MM.

The simulated total efficiency versus frequency graph of antenna with and without MM are shown in Fig. 11. The total efficiency of antenna with and without MM varies between 60 and 90% and between 37 and 80%, respectively, within the operational bandwidth. Its total efficiency is decreased when the metamaterial is integrated with the antenna. The decrease in efficiency has increased in resonance frequencies of MM. This reduction in efficiency can be attributed to impedance matching and thermal (dielectric and surface wave) losses.

In Fig. 12, the simulated front-to-back ratio (FBR) versus frequency graph of the antenna is given comparatively, with and without MM. The simulated FBR for the proposed antenna without MM varies between − 4.4 and 11 dB over the entire operating frequency band of 3–16 GHz whereas the simulated FBR for antenna with MM layers varies between 5 and 26.6 dB. The FBR of antenna with MM is increased over the entire operating frequency band. The integration of MM into the antenna has reduced the backward radiation of the antenna and increased the forward radiation of the antenna. Thus, it is clear that after adding the MM to the antenna, the FBR and gain are significantly increased. These results showed that, the proposed antenna with MM provides advantages for WBAN applications.
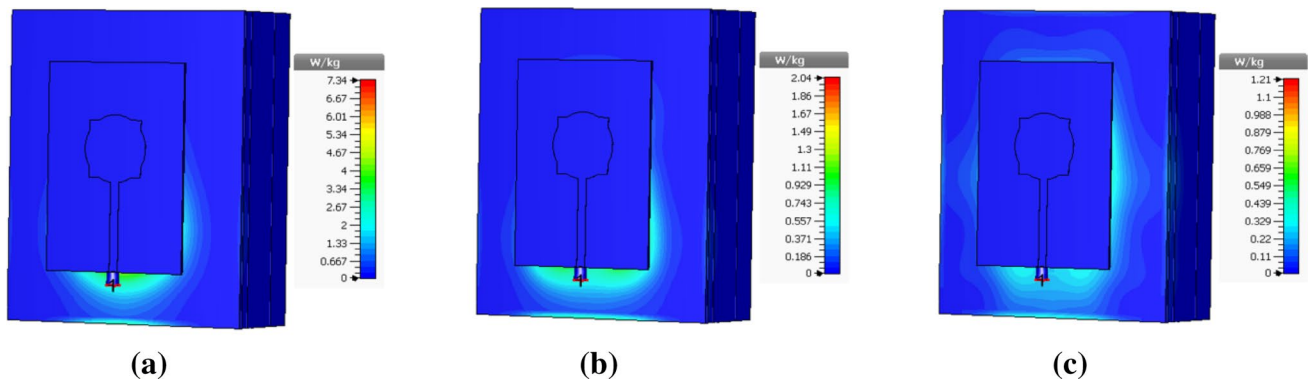
Fig. 13 Simulated SAR of the design antenna without MM for 10 g standard; **a** 4 GHz; **b** 7 GHz; **c** 10 GHz
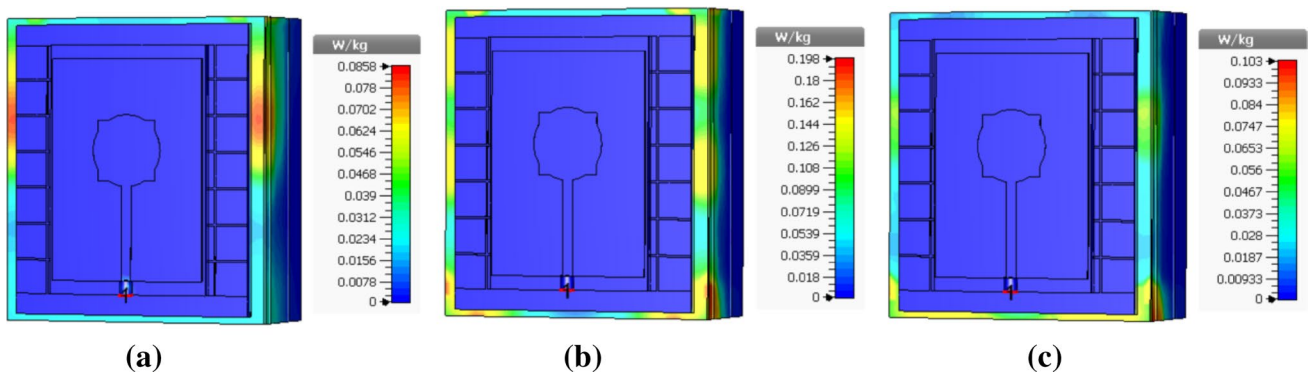
Fig. 14 Simulated SAR of the design antenna with MM for 10 g standard; **a** 4 GHz; **b** 7 GHz; **c** 10 GHz

Table 2 The SAR analysis summary of wearable antenna [10 g tissue standard SAR (W/kg)]

Antenna condition	Frequencies		
	4 GHz	7 GHz	4 GHz
Antenna without MM	7.34 W/kg	Antenna without MM	7.34 W/kg
Antenna with MM	0.086 W/kg	Antenna with MM	0.086 W/kg

3.4 Specific absorption rate (SAR) analysis of antenna with and without metamaterial

The SAR value of the antenna with and without MM on the body model was simulated and evaluated according to the International Commission of Non-Ionization Radiation Protection (ICNIRP) for Europe's standards. The antenna input power is 0.5 W. The distance between the antenna and the body model was kept constant to compare the SAR values of the antenna with and without MM. This distance is 6.9 mm as the sum of the MM and interlayer thickness. The peak SAR results of the simulation of the only antenna on the body model are given in Fig. 13. The Simulated

peak SAR values when the antenna without MM was placed on the body model are 7.34, 2.04, and 1.21 W/kg at frequencies of 4 GHz, 7 GHz, and 10 GHz, respectively, for 10 g of tissue (safety limit is 2 W/kg for 10-g tissue). As shown in Fig. 14, the simulated peak SAR values when the antenna with MM was placed on the body model are 0.086, 0.198, and 0.103 W/kg at frequencies of 4 GHz, 7 GHz, and 10 GHz, respectively, for 10 g of tissue. Peak SAR values of antenna without MM have been observed to be high according to European standards (safety limit 10 g for tissue 2 W/kg). SAR values of antenna with MM were observed to be quite low and appropriate to European standards. The simulated peak SAR value of the antenna with MM is also reduced by 97%, compared to the simulated peak SAR value of the antenna without MM (Table 2).

A comparison between the proposed antenna with MM and reference antennas with MM in literature is given in Table 3 for the operating frequency bandwidth, flexibility, footprint, thickness (low-profile), and gain characteristics. The design presented in the table appears to be very advantageous in terms of gain and bandwidth. The studies in [32, 37, 38], whose gain is slightly higher than the proposed

Table 3 Comparison of proposed and reference antennas with MMs

References	Operating band (GHz)	Substrate type (flexible/rigid)	MM dimensions (mm)	Thickness of Antenna with MM (mm)	Peak Gain (dB/dBi)
[40]	2.4 ISM	Flexible	50×50×3	9.5	4.12 dBi
[41]	2.3–3/4–5.3	Flexible	77×87×4	8	7.3 dB
[42]	2.45/ 5.5	Flexible	102×102×3	7	5.2 dB
[37]	3.5–7	N/a	90×90×3	31.8	10.6 dB
[32]	5.75–14.51	Rigid	50×80×2.4	4	10.65 dBi
[33]	5.7–11	Flexible	46×46×3.5	5.8	8 dBi
[39]	4.2–8.1	Rigid	88×75×3.2	5.78	7.9 dB
[38]	2.6–12	Rigid	72×72×3.2	14.8	9.9 dBi
[43]	2.45 /5.8	Flexible	42×63	8	7.8 dB
[34]	2.5–13.8	Flexible	52.5×52.5×5	20	9 dB
Proposed	3.5–12.4	Flexible	91×105×3.6	7.9	9.1 dB

design, are unsuitable for wearable antennas since they are rigid (additionally [39]) and high-profile structures. Other studies in [33, 34, 40–43] are presented by the authors for wearable applications. The study in [34] has a wider bandwidth than the proposed design, but it is the biggest disadvantage for wearable applications due to its relatively high-profile construction. As can be seen from the ref [32, 34, 38], it is very difficult to design low-profile UWB antenna with integrated MM. The proposed antenna offers advantages in terms of bandwidth, footprint, low profile and gain than wearable Ref. [33, 40–43], Ref. [42], Ref. [34, 40, 41, 43], Ref. [33, 34, 40–43], respectively. Since the proposed antenna is within the thickness and footprint dimensions of the antennas offered by the authors for WBAN, its slightly larger dimensions will not be a huge problem. The table reveals that especially when all of these characteristic features are evaluated together, the proposed antenna is a better performance according to the previously proposed antenna structures.

4 Conclusions

In this study, an ultra-wide band low-specific absorption rate (SAR) flexible metasurface-enabled wearable antenna is proposed. The results of the simulated and measured impedance matching performance reflection coefficient parameter have shown that the planar antenna with MM in free space has a wide frequency bandwidth, which covers the UWB frequency band. A MM structure is designed to increase the radiation performance parameters of the antenna and to reduce the interaction between the human body and the antenna. The impedance matching characteristics and SAR values of designed antenna with and without MM have been successfully obtained with CST simulation program in free space and on the

body. Especially on the side of the low frequency band, the directivity of the antenna is increased and due to this, the back radiation and SAR values have decreased. Moreover, when the antenna is placed on the MM, it provides a stable impedance matching in free space and on the body. Peak SAR values are well below the 2 W/kg European safety limitations. The simulated maximum SAR value of the antenna with MM is also reduced by 97%, compared to the simulated maximum SAR value of the antenna without MM. The realized peak gain of the antenna is significantly increased from 4.6 to 9.1 dB by the MM. As a result of this study, MM integrated compact, UWB, low SAR, and high directivity flexible wearable antenna has been successfully designed and fabricated for WBAN applications. These features provide significant advantages for WBAN applications. It is evaluated that the study and its results will make a significant contribution to the literature for the UWB MM antennas and shed light on the antenna designers.

References

1. M.A.B. Abbasi, S.S. Nikolaou, M.A. Antoniades, M.N. Stevanović, P. Vryonides, Compact EBG-backed planar monopole for BAN wearable applications. IEEE Trans. Antennas Propag. **65**(2), 453–463 (2017)
2. S.M. Saeed, C.A. Balanis, C.R. Birtcher, A.C. Durgun, H.N. Shaman, Wearable flexible reconfigurable antenna integrated with artificial magnetic conductor. IEEE Antennas Wirel. Propag. Lett. **16**, 2396–2399 (2017)
3. D. Chaturvedi, S. Raghavan, Circular quarter-mode SIW antenna for WBAN application. IETE J. Res. **64**(4), 482–488 (2018)

4. G.-P. Gao, B. Hu, S.-F. Wang, C. Yang, Wearable circular ring slot antenna with EBG structure for wireless body area network. IEEE Antennas Wirel. Propag. Lett. **17**(3), 434–437 (2018)

5. G. Gao, B. Hu, S. Wang, C. Yang, Wearable planar inverted-F antenna with stable characteristic and low specific absorption rate. Microw. Opt. Technol. Lett. **60**(4), 876–882 (2018)

6. C. Mendes, C. Peixeiro, A dual-mode single-band wearable microstrip antenna for body area networks. IEEE Antennas Wirel. Propag. Lett. **16**, 3055–3058 (2017)

7. Z.H. Jiang, D.E. Brocker, P.E. Sieber, D.H. Werner, A compact, low-profile metasurface-enabled antenna for wearable medical body-area network devices. IEEE Trans. Antennas Propag. **62**(8), 4021–4030 (2014)

8. F. Wan, J. Chen, B. Li, A novel ultra-wideband antipodal Vivaldi antenna with trapezoidal dielectric substrate. Microw. Opt. Technol. Lett. **60**(2), 449–455 (2018)

9. V. Kumar, B. Gupta, Swastika slot UWB antenna for body-worn application in WBAN, in *Medical Information and Communication Technology (ISMICT), 2014 8th International Symposium on, IEEE*, 2014, pp. 1–5

10. L.A.Y. Poffelie, P.J. Soh, S. Yan, G.A. Vandenbosch, A high-fidelity all-textile UWB antenna with low back radiation for off-body WBAN applications. IEEE Trans. Antennas Propag. **64**(2), 757–760 (2016)

11. U.F.C. Commission, *FCC Revision of Part 15 of the Commission's Rules Regarding Ultra-Wideband Transmission Systems: First Report and Order, technical report,* Feb, 2002

12. M. Shakhirul, M. Jusoh, A. Ismail, M. Jais, M. Kamarudin, M. Osman, *Analysis of circular polarization textile antenna in bending condition, Computer, Communications, and Control Technology (I4CT), 2015 International Conference on, IEEE*, 2015, pp. 360–363.

13. M.E. Lajevardi, M. Kamyab, Ultraminiaturized metamaterial-inspired SIW textile antenna for off-body applications. IEEE Antennas Wirel. Propag. Lett. **16**, 3155–3158 (2017)

14. W.A.M. Al Ashwal, K.N. Ramli, *Compact UWB wearable Antenna with İmproved Bandwidth and Low SAR, RF and Microwave Conference (RFM), 2013 IEEE International, IEEE*, 2013, pp. 90–94

15. A. da Conceicao Andrade, I. P. Fonseca, S. F. Jilani, and A. Alomainy, *Reconfigurable textile-based ultra-wideband antenna for wearable applications. In: 2016 10th European Conference on Antennas and Propagation (EuCAP) IEEE,* 2016, pp. 1–4.

16. M. Koohestani, N. Pires, A.K. Skrivervik, A.A. Moreira, *Influence of the human body on a new coplanar-fed ultra-wideband antenna, Antennas and Propagation (EUCAP), 2012 6th European Conference on, IEEE,* 2012, pp. 316–319.

17. K. Kamardin, M.K.A. Rahim, P.S. Hall, N.A. Samsuri, T.A. Latef, M.H. Ullah, Textile artificial magnetic conductor jacket for transmission enhancement between antennas under bending and wetness measurements. Appl. Phys. A **122**(4), 423 (2016)

18. U. Ali, S. Ullah, J. Khan, M. Shafi, B. Kamal, A. Basir, J.A. Flint, R.D. Seager, Design and SAR analysis of wearable antenna on various parts of human body, using conventional and artificial ground planes. J. Electr. Eng. Technol. **12**(1), 317–328 (2017)

19. Z.H. Jiang, D.H. Werner, *Robust low-profile metasurface-enabled wearable antennas for off-body communications, Antennas and Propagation (EuCAP), 2014 8th European Conference on, IEEE,* 2014, pp. 21–24.

20. M. Koohestani, J.-F. Zürcher, A.A. Moreira, A.K. Skrivervik, A novel, low-profile, vertically-polarized UWB antenna for WBAN. IEEE Trans. Antennas Propag. **62**(4), 1888–1894 (2014)

21. S. Yan, P.J. Soh, G.A. Vandenbosch, Wearable dual-band magneto-electric dipole antenna for WBAN/WLAN applications. IEEE Trans. Antennas Propag. **63**(9), 4165–4169 (2015)

22. M. Hossain, M. Faruque, M. Islam, M. Ali, Low-SAR metamaterial-inspired printed monopole antenna. Appl. Phys. A **123**(1), 87 (2017)

23. A. Alemaryeen, S. Noghanian, Crumpling effects and specific absorption rates of flexible AMC integrated antennas. IET Microw. Antennas Propag. **12**(4), 627–635 (2017)

24. F.N. Giman, P.J. Soh, M.F. Jamlos, H. Lago, A.A. Al-Hadi, M. Abdulmalek, N. Abdulaziz, Conformal dual-band textile antenna with metasurface for WBAN application. Appl. Phys. A **123**(1), 32 (2017)

25. Y.-W. Huang, W.T. Chen, P.C. Wu, V. Fedotov, V. Savinov, Y.Z. Ho, Y.-F. Chau, N.I. Zheludev, D.P. Tsai, Design of plasmonic toroidal metamaterials at optical frequencies. Opt. Express **20**(2), 1760–1768 (2012)

26. Y.-F.C. Chau, J.-Y. Syu, C.-T.C. Chao, H.-P. Chiang, C.M. Lim, Design of crossing metallic metasurface arrays based on high sensitivity of gap enhancement and transmittance shift for plasmonic sensing applications. J. Phys. D Appl. Phys. **50**(4), 045105 (2016)

27. Y.-F.C. Chau, C.-T.C. Chao, J.-Y. Rao, H.-P. Chiang, C.M. Lim, R.C. Lim, N.Y. Voo, Tunable optical performances on a periodic array of plasmonic bowtie nanoantennas with hollow cavities. Nanoscale Res. Lett. **11**(1), 411 (2016)

28. M. Grelier, F. Linot, A. Lepage, X. Begaud, J. LeMener, M. Soiron, Analytical methods for AMC and EBG characterizations. Appl. Phys. A **103**(3), 805–808 (2011)

29. Y.-F.C. Chau, J.-C. Jiang, C.-T.C. Chao, H.-P. Chiang, C.M. Lim, Manipulating near field enhancement and optical spectrum in a pair-array of the cavity resonance based plasmonic nanoantennas. J. Phys. D Appl. Phys. **49**(47), 475102 (2016)

30. N. Kumara, Y.-F.C. Chau, J.-W. Huang, H.J. Huang, C.-T. Lin, H.-P. Chiang, Plasmonic spectrum on 1D and 2D periodic arrays of rod-shape metal nanoparticle pairs with different core patterns for biosensor and solar cell applications. J. Opt. **18**(11), 115003 (2016)

31. H.-L. Yang, H. Wao, Y. Yi, X. Huang, S. Wu, B. Xiao, A dual-band low-profile metasurface-enabled wearable antenna for WLAN devices. Progress Electromagn. Res. C **61**, 115–125 (2016)

32. H. Malekpoor, S. Jam, Improved radiation performance of low profile printed slot antenna using wideband planar AMC surface. IEEE Trans. Antennas Propag. **64**(11), 4626–4638 (2016)

33. X. Liu, Y. Di, H. Liu, Z. Wu, M.M. Tentzeris, A planar windmill-like broadband antenna equipped with artificial magnetic conductor for off-body communications. IEEE Antennas Wirel. Propag. Lett. **15**, 64–67 (2016)

34. F. Wang, T. Arslan, A wearable ultra-wideband monopole antenna with flexible artificial magnetic conductor, in *Antennas & propagation conference (LAPC), 2016 Loughborough, IEEE*, 2016, pp. 1–5

35. S. Shahid, M. Rizwan, M. Abbasi, M. Tarar, S. Abbas, Bend Profiling of textile antenna for body centric wireless communication (pre published copy 2014).

36. CST MWS https://www.cst.com/products/cstemcs/solvers Accessed 18 Feb 2019.

37. K. Agarwal, Y.-X. Guo, B. Salam, Wearable AMC backed near-endfire antenna for on-body communications on latex substrate. IEEE Trans. Compon. Packag. Manuf. Technol. **6**(3), 346–358 (2016)

38. M. Mantash, A.-C. Tarot, S. Collardey, K. Mahdjoubi, Investigation of lexible textile antennas and AMC relectors. Int. J. Antennas Propag. **2012**, 1–10 (2012)

39. N. Chahat, M. Zhadobov, R. Sauleau, K. Mahdjoubi, Improvement of the on-body performance of a dual-band textile antenna using an EBG structure, in *Antennas and Propagation Conference (LAPC), 2010 Loughborough, IEEE,* 2010, pp. 465–468

40. P. Prakash, M.P. Abegaonkar, A. Basu, S.K. Koul, Gain enhancement of a CPW-fed monopole antenna using polarization-insensitive AMC structure. IEEE Antennas Wirel. Propag. Lett. **12**, 1315–1318 (2013)

41. C. Joshi, A.C. Lepage, J. Sarrazin, X. Begaud, Enhanced broadside gain of an ultrawideband diamond dipole antenna using a hybrid reflector. IEEE Trans. Antennas Propag. **64**(7), 3269–3274 (2016)

42. G. Kumar Pandey, H. Shankar Singh, M. Kumar Meshram, Investigations of triple band artificial magnetic conductor back plane with UWB antenna, Microw. Opt. Technol. Lett. **58**(8), 1900–1906 (2016)

43. A. Mersani, O. Lotfi, J.M. Ribero, Design of a textile antenna with artificial magnetic conductor for wearable applications. Microw. Opt. Technol. Lett. **60**(6), 1343–1349 (2018)